Double K-shell vacancy production in the electron capture decay of ^{139}Ce

M.M. Hindi and R.L. Kozub
Physics Department, Tennessee Technological University, Cookeville, Tennessee 38505
(Received 3 August 1990)

The probability of double K-shell vacancy production in the electron capture decay of ^{139}Ce to the 166-keV level of ^{139}La has been investigated. Triple coincidences between the 166-keV gamma ray, the La satellite $K\alpha$ x ray, and the La hypersatellite $K\alpha$ x ray were measured using two intrinsic Ge detectors. We looked for the sum of two of the three radiations in one detector in coincidence with the third radiation in the other detector. The probability of double K-shell vacancy production per K-shell electron capture (P_{KK}) was found to be $(2.0 \pm 1.6) \times 10^{-6}$. From this and the known P_{KK} for ^{131}Cs we estimate a probability for zero K-shell vacancy production (shakedown) per K-shell electron capture of $\lesssim 2.4 \times 10^{-5}$ for ^{139}Ce.

I. INTRODUCTION

When a nucleus decays by capturing an electron from the K shell the sudden change of the nuclear charge from Ze to $(Z-1)e$ and the concomitant disappearance of the electron can cause the remaining electron in the K shell to be excited to unoccupied levels (shakeup, SU) or to continuum states (shakeoff, SO), thus leaving a double vacancy in the shell. In quantum-mechanical terms, the Hamiltonian changes in a nonadiabatic way and hence the initial electron wave function can go into any one of the eigenstates of the final Hamiltonian (subject, of course, to the Pauli exclusion principle). The process has been observed in the electron capture (EC) decay of several isotopes and a number of theoretical calculations of P_{KK}, the probability of double K-shell vacancy production per K-electron capture, have been reported.[1] In Table I we compare various theories with recent experimental results for all 13 isotopes for which measurements of P_{KK} have been made. A cursory inspection of the table reveals the following: (1) disagreements among the various theories range from ~25% to a factor of 20, (2) most of the experimental results lie somewhere between the various theoretical calculations and do not clearly favor one calculation over another, and (3) the experimental results have large errors (10%–50%), and, more importantly, there are serious disagreements among different measurements on the same isotope in several cases. Clearly, a quantitative understanding of the phenomenon is still lacking, and there is a definite need for further theoretical and experimental work. In this paper we report a measurement of the probability for double K-shell ionization in the electron capture decay of ^{139}Ce (decay scheme shown in Fig. 1), using a sum-coincidence technique which has not been utilized in such studies before.

Experiments to measure P_{KK} usually record coincidences between the hypersatellite ($K\alpha^H$) and satellite ($K\alpha^S$) x rays produced in the transitions $1s^{-2} \rightarrow 1s^{-1}2p^{-1}$ and $1s^{-1}2p^{-1} \rightarrow 2p^{-2}$, respectively. However, owing to the small probability with which the process happens ($\sim 10^{-5}$ per K capture), the experiments are difficult and events can be obscured by coincidences between x rays and Compton tails of γ rays, and by coincidences between x rays produced in EC and x rays associated with the internal conversion (IC) of excited nuclear states. As a result, most experiments have been performed on isotopes which decay exclusively to the ground state of the daughter (^{37}Ar, ^{55}Fe, ^{71}Ge, ^{131}Cs, ^{165}Er) or to an isomeric excited state (^{85}Sr, ^{103}Pd, ^{109}Cd). In the case of decay to a metastable state which has a substantial internal conversion coefficient, subsidiary experiments have to be conducted to determine the contribution of double K-shell ionization arising from IC of the metastable state (^{109}Cd).[14] Cases of decay to nonisomeric excited states have been studied,[5,8] but the excited states had to have negligible IC coefficients and the γ rays had to be energetic enough so as to have a small chance of producing a Compton event in the detectors. In view of these restrictions, it is not surprising that the number of reliable experimental results are few. We have begun a program of research utilizing a technique which will allow us to measure P_{KK} for several isotopes that have decays to nonisomeric excited states with non-negligible IC coefficients, thus enabling us to extend the base of experimental systematics. The first of these measurements is reported herein.

In addition to contributing to the systematics of double K-shell ionization, the measurement of P_{KK} for ^{139}Ce provides information which is needed for the proper interpretation of a recent measurement by Schupp, Nagy, and Miles[21] of the probability per K internal conversion of double K-shell ionization, P_{KK}(IC), accompanying the internal conversion of the 166-keV transition in ^{139}La. These authors measured P_{KK}(IC) by recording triple coincidences between the normal La $K\alpha^N$ x ray accompanying the filling of the vacancy produced in K-electron capture, and the subsequent La $K\alpha^H$ and $K\alpha^S$ x rays accompanying the filling of the double vacancy produced

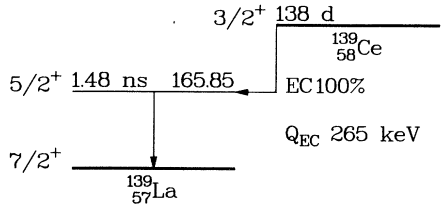

FIG. 1. Decay scheme of ^{139}Ce. The level energy is in keV.

in the K internal conversion of the 166-keV transition. However, as the authors note, triple coincidences can also result from hypersatellite and satellite x rays produced from double ionization accompanying EC with a normal x ray produced after IC of the 166-keV level. They do not subtract the contribution of such events from their data because the theories of Suzuki and Law[3] (SL) and Intemann[1] predict P_{KK}(EC) for ^{139}Ce to be 8.4×10^{-7} and 2.6×10^{-7}, respectively;[22] these values are about 10^{-2} smaller than the measured value of $(6.0 \pm 1.4) \times 10^{-5}$ which Schupp *et al.* ascribe to P_{KK}(IC). As shown in Table I, the SL theory underestimates the two discordant measurements of P_{KK} of ^{181}W by factors of 1.7 ± 0.4 and 9 ± 3. Of all the isotopes for which P_{KK}(EC) has been measured, ^{181}W has the lowest Q value for double K-shell ionization. The next lowest Q value is for ^{109}Cd, and there, too, SL is on the low side of the experimental values. So the question arises as to whether the SL theory underestimates P_{KK} for decay energies near threshold. Since ^{139}Ce has an even lower Q value for double K-shell ionization than ^{181}W, there is a possibility that the SL theory underestimates P_{KK} for ^{139}Ce as well. Hence, to provide an experimental basis for the assumptions of Ref. 21 and to test the extent of discrepancy with the SL theory, a measurement of P_{KK}(EC) for ^{139}Ce is desirable.

II. EXPERIMENTAL PROCEDURE

Our experimental technique consisted of measuring triple coincidences between the two x rays and the γ ray from the decay of the excited nuclear state. The coincidences were measured using two detectors; we looked for the sum of two of the three radiations in one detector in coincidence with the third radiation in the other detector. The detection of the full energy of the γ ray insured that the x rays were not associated with IC of the nuclear state and that the coincidence was not between an x ray and the Compton tail of the γ ray.

Sources of approximate strengths 10–40 nCi were prepared by evaporating several drops of an active solution of $CeCl_3$ in 1 N HCl onto cellophane tape, and sealing the dried tape with a similar piece. These sources were sandwiched between two intrinsic Ge (Gamma-X) detectors

TABLE I. Comparison of various theories with recent experimental results.

Nuclide	$10^5 P_{KK}$ MIKS[a]	Intemann[b]	SL[c]	Expt.	Ref.
^{37}Ar	23.0	25.84	52.94	37±9	4
^{54}Mn		11.25	24.3	36±3	5
^{55}Fe	15.8	9.42	20.1	12±4	6
				10.1±2.7	7
^{65}Zn			15.3	22±2	8
^{71}Ge	8.85	5.08	11.84	12	9
^{85}Sr		3.38	9.38	6.0±0.5	10
^{103}Pd		1.74	6.03	3.13±0.31	11
^{109}Cd		0.34	0.89	15.2±2.4	12
				2.8±0.7	13
				1.02±0.36	14
^{113}Sn		1.34	5.33	1.5±0.5	15
^{131}Cs	1.79	0.75	3.22	1.33±0.33	16
				2.3±0.3	17
				1.4±0.1	18
^{165}Er	1.09	0.26	1.71	0.67±0.39	16
				0.82±0.28	19
^{181}W		0.022	0.14	0.24±0.06	19
				1.25±0.42	15
^{207}Bi		0.11	1.97	0.6±0.25	20

[a] Reference 2.
[b] Reference 1.
[c] Reference 3.

placed face to face. One of the detectors had a 43.5 mm diameter, 45.3 mm depth, and 3 mm window-to-endcap distance, and the other a 54.2 mm diameter, 39.2 mm depth, and 5 mm window-to-endcap distance. Both detectors had 0.5 mm Be windows; these were thick enough to stop Auger and conversion electrons associated with ^{139}Ce decay. The resolution of the detectors at the La $K\alpha$ line ($\approx$ 33 keV) was 715 eV.

The detectors were connected to amplifiers equipped with pileup rejection circuitry. A standard circuit was used to generate coincidence signals. The energy and fast-timing signals (described below) from each detector were digitized in two analog-to-digital converters (ADC's) and an eight-channel time-to-digital converter (TDC) in a CAMAC crate interfaced to a VAX 11/725 computer. The digitized signals and a word tagging pileup events were recorded event by event on magnetic tape for later analysis. Most of the recorded data consisted of coincidence events only, with singles-plus-coincidence data recorded in short runs every few days. The total counting time was approximately 90 days.

The sum-coincidence method utilized in this study presents a problem not found in typical coincidence measurements: accidental $(\gamma+K\alpha)\otimes K\alpha$ and $\gamma\otimes(K\alpha+K\alpha)$ coincidences can be generated by a true $\gamma\otimes K\alpha$ coincidence followed by an accidental $K\alpha$ which piles up into one of the two detectors, or by a true $K\alpha\otimes K\alpha$ coincidence followed by an accidental γ. The rate of such accidentals is determined by the resolving time of the pileup rejection circuitry. The pileup rejection circuitry of the ORTEC 572 amplifiers which we used have a resolving time of approximately 650 ns, which is much wider than our fast-time window of 180 ns. The integration time constant we used in the amplifiers was 6 μs; thus accidental pulses less than 650 ns apart give virtually the same energy signal as a true sum-coincidence peak. The pileup rejection circuitry of the amplifiers was thus ineffective for sum-coincidence work.

Our partial solution to this problem was to measure the risetime of each pulse by feeding a pulse from a fast-timing filter amplifier (TFA) to two leading-edge (LE) modules, one set at a low threshold T_l and the other set at a higher threshold T_h, as shown in Fig. 2(a). As depicted schematically in Fig. 2(b), the time t_r that a pulse takes to rise from T_l to T_h depends inversely on its amplitude. If two low-amplitude pulses pileup in the detector, t_r will be determined by the pulse that came first. This holds true as long as the second pulse comes after the first has reached T_h. The high threshold was set so that this time was on the order of 100 ns, while the low threshold was set at approximately one-half the high threshold. The fast-timing signal generated by the LE module when the pulse from one of the detectors reached T_l served as the start for the TDC, while the fast-timing signal generated at T_h, and the fast timing signals generated when the pulse from the other detector reached T_l and T_h served, after appropriate delays, as the stop signals for three out of the eight available channels on the TDC.

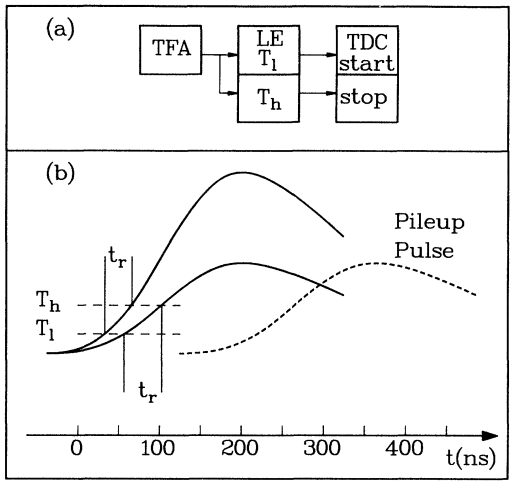

FIG. 2. (a) Schematic diagram of the fast-timing circuit used to improve pileup rejection. (b) Schematic illustration of the working principle of the circuit: If a pileup pulse follows a low-amplitude pulse, t_r will be determined by the first pulse and thus be longer than the t_r for a single pulse having the same total amplitude.

Figure 3 shows a two-dimensional (2D) t_r-E_γ density plot for events in coincidence with the 166-keV γ ray. The most intense peak in the spectrum corresponds to $K\alpha$'s in true coincidence with the γ ray. Other events follow two almost distinct loci, one with t_r decreasing as E_γ increases, as would be expected for pulses with increasing amplitudes, and the other with t_r constant at a value equal to that for $K\alpha$ (45 ns), as would be expected for pulses piling up onto the $K\alpha$ pulse. During event replay from magnetic tape a 2D software gate that

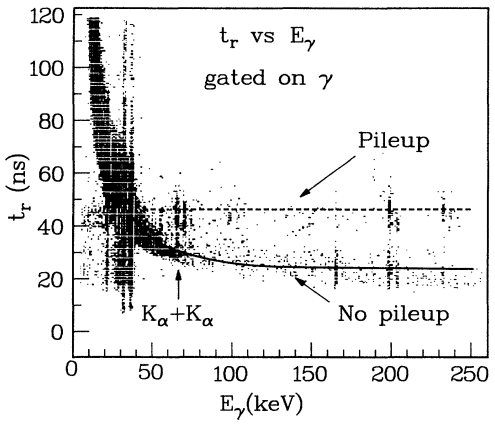

FIG. 3. A sample two dimensional t_r-E_γ density plot for events in coincidence with the 166-keV γ ray. The solid line shows the locus of no-pileup events; the dashed line shows the locus of pileup with K x rays.

encloses the first locus selected the no-pileup events. (Of course, there is still pileup in those "no-pileup" events for pulses coming less than 100 ns apart.) It is clear from Fig. 3 that true $K + K$ events can be separated from pileup $K + K$ events. However, the difference in t_r between a γ pulse and a $\gamma + K$ pulse is insufficient to distinguish between true and pileup $\gamma + K$. Hence we succeeded in reducing pileup for events in which a true K is followed by a pileup K or a pileup γ, but not for those in which a true γ is followed by a pileup K. Thus $\gamma \otimes (K + K)$ events have substantially reduced pileup, while $K \otimes (\gamma + K)$ events have reduced $K_{\text{true}} \otimes (K_{\text{true}} + \gamma_{\text{pileup}})$ events, but not $K_{\text{true}} \otimes (\gamma_{\text{true}} + K_{\text{pileup}})$ events.

III. DATA ANALYSIS AND RESULTS

The data on the magnetic tapes were replayed to generate singles and coincidence spectra which satisfied the following requirements: (1) no pileup signal generated by the amplifier, (2) the pair (E_γ, t_r) passed through a 2D software gate around the locus expected for no-pileup events (see Fig. 3), and (3) the time difference between the fast signals passed through a gate set on the prompt peak. In addition, we took advantage of the event-by-event recording of the data to compensate for slow drifts in the energy signals as follows: The change in the centroids of the $K\alpha$ and 166-keV peaks was obtained from the raw data every 5×10^4 counts (equivalent to counting for approximately two hours) and a corrected energy signal was computed based on that change.

Sample singles and coincidence spectra are shown in Fig 4. All lines in these spectra are due to ^{139}Ce decay; the lines are the La L, $K\alpha$, and $K\beta$ x rays, the 166-keV γ ray, Ge $K\alpha$ escape lines, and lines due to sums of the aforementioned radiations. In addition, Pb x rays due to absorption of the 166-keV γ ray in the lead shielding surrounding the detectors are clearly visible in the 70–90-keV region, especially in the coincidence spectrum gated on La $K\alpha$. There was no evidence for any contaminants in the source.

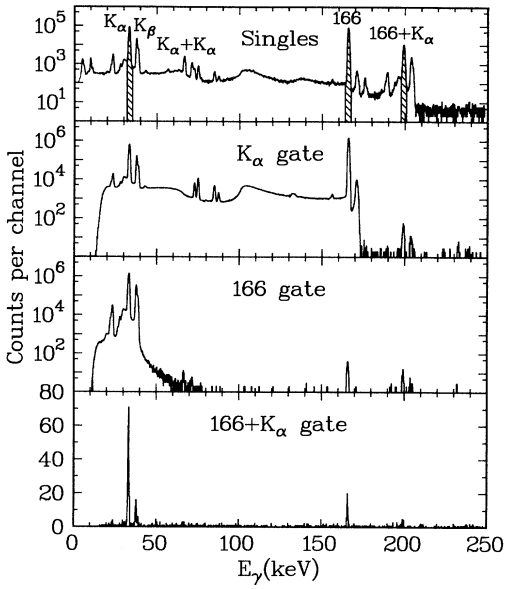

FIG. 4. Sample singles and gated coincidence spectra from the EC decay of ^{139}Ce. The gates were set on the shaded peaks. The K x rays belong to La.

We can, in principle, extract P_{KK} from any one of the following six coincidence peaks: $(K\alpha^H)_1 \otimes (K\alpha^S + \gamma)_2$, $(K\alpha^S)_1 \otimes (K\alpha^H + \gamma)_2$, $(\gamma)_1 \otimes (K\alpha^H + K\alpha^S)_2$, $(K\alpha^S + \gamma)_1 \otimes (K\alpha^H)_2$, $(K\alpha^H + \gamma)_1 \otimes (K\alpha^S)_2$, and $(K\alpha^H + K\alpha^S)_1 \otimes (\gamma)_2$, where γ denotes the 166-keV γ ray. The subscripts 1 and 2 refer to detectors one and two, respectively. The number of triple coincidences, say $N[(\gamma)_1 \otimes (K\alpha^H + K\alpha^S)_2]$, is related to P_{KK} by

$$N[(\gamma)_1 \otimes (K\alpha^H + K\alpha^S)_2] = N_0 P_K P_{KK} \left[\left(\frac{\gamma}{T}\right)(\epsilon_\gamma)_1\right] \left[\omega_K^H \left(\frac{K\alpha}{K_T}\right)^H (\epsilon_{K\alpha^H})_2\right] \left[\omega_K^S \left(\frac{K\alpha}{K_T}\right)^S (\epsilon_{K\alpha^S})_2\right] \epsilon_c , \quad (1)$$

where N_0 is the number of ^{139}Ce EC decays, P_K the fraction of K-capture decays, (γ/T) the fraction of radiative decays of the 166-keV level; ω_K^H and ω_K^S are the fluorescence yields, respectively, of La K^H and K^S x rays; $(K\alpha/K_T)^H$ and $(K\alpha/K_T)^S$ are, respectively, the fractions of hypersatellite and satellite $K\alpha$ x rays; $(\epsilon_\gamma)_1$, $(\epsilon_{K\alpha^H})_2$, and $(\epsilon_{K\alpha^S})_2$ are the absolute efficiencies for detecting the respective radiations in detectors 1 and 2, and ϵ_c is the coincidence efficiency, which is the fraction of real coincidence events selected by the risetime and fast-timing software gates.

The number of recorded $(\gamma)_1 \otimes (K\alpha^N)_2$ double coincidences is given by

$$N[(\gamma)_1 \otimes (K\alpha^N)_2] = N_0 P_K \left[\left(\frac{\gamma}{T}\right)(\epsilon_\gamma)_1\right] \times \left[\omega_K \left(\frac{K\alpha}{K_T}\right)(\epsilon_{K\alpha})_2\right] \epsilon_c, \quad (2)$$

where $K\alpha^N$ refers to a normal $1s^{-1} \rightarrow 2p^{-1}$ x ray. One can then obtain P_{KK} by dividing Eq. (1) by Eq. (2) and rearranging. We simplify the result by noting that $\epsilon_{K\alpha^H} = \epsilon_{K\alpha^S} = \epsilon_{K\alpha}$ to better than 1%, and that[23] $\omega_K^H \simeq \omega_K^S \simeq \omega_K$ [=0.906 (Ref. 24)]. As noted by Åberg,[25] the intensity ratio $(K\alpha_1/K\alpha_2)$ is smaller for hypersatellite x rays than for normal x rays. Schupp *et al.*[21] assume that this also leads to a reduction in $(K\alpha/K_T)^H$; however, the calculations of Chen, Crasemann, and Mark,[23] and the measurement of Isozumi *et al.*[18] on ^{131}Cs show that the ratio $(K\alpha/K_T)^H$ is essentially the same as that for normal lines. Therefore we take $(K\alpha/K_T)^H = (K\alpha/K_T)^S = (K\alpha/K_T)$ [= 0.807 (Ref. 24)]. With these simplifications P_{KK} can be obtained as

$$P_{KK} = \frac{N[(\gamma)_1 \otimes (K\alpha^H + K\alpha^S)_2]}{N[(\gamma)_1 \otimes (K\alpha^N)_2]} \frac{1}{\omega_K (K\alpha/K_T)(\epsilon_{K\alpha})_2} . \quad (3)$$

We note here that (γ/T) depends on the number of electrons in the K shell and, in principle, the (γ/T) appearing in Eq. (1) should be different from that appearing in Eq. (2). However, the atomic half-lives of the single and double holes in the K shell are on the order of 10^{-16} s (Ref. 23), which is much shorter than the 1.48 ns half-life of the 166-keV level. Hence the holes are nearly always filled by the time the 166-keV level decays, and (γ/T) is essentially the same for double and triple coincidences.

Similar expressions relate P_{KK} to the other five coincidence peaks. Since the two detectors had equal gains and resolutions, we added the two spectra (one from each detector) gated on the $K\alpha$'s, the two gated on the γ's, and the two gated on the $K\alpha + \gamma$'s, to obtain a total of three different spectra. The expressions for P_{KK} were modified appropriately to take into account the different efficiencies of the two detectors.

As shown in Fig. 5, the $K\alpha$ region of the spectrum gated on the $(K\alpha + \gamma)$ sum peak is dominated by $K\alpha^N$ x rays. These $K\alpha^N$ x rays arise mostly from $K^N_{\text{true}} \otimes (\gamma_{\text{true}} + K^N_{\text{pileup}})$ coincidences, and, to a much lesser extent, from accidental coincidences of $K\alpha^N$ x rays with true $(\gamma + K\alpha^N)$ sums. True coincidences between $K\alpha^N$ x rays and the sum of the 166-keV γ ray with internal bremsstrahlung (IB) accompanying K capture are negligible. Using the semirelativistic expressions given by Bambynek *et al.*,[26] we estimate the yield of $1s$ IB radiation in the range 30–35 keV to be 2×10^{-7} per K capture, which would account for only 0.1% of the observed $K\alpha^N$ counts. Indeed, the spectrum gated on $K\alpha$ (Fig. 4), shows very little continuum radiation in the region of the $166 + K\alpha$ peak.

The yield of $K\alpha^H$ x rays was extracted from the spectrum shown in Fig. 5 by fitting the $K\alpha$ region with four Gaussians superimposed on a linear background. Two of the Gaussians corresponded to $K\alpha_1^N$ and $K\alpha_2^N$ x rays and the other two corresponded to $K\alpha_1^H$ and $K\alpha_2^H$. In this fit we have neglected the $K\alpha^S$ peaks; it is clear from Fig. 5 that the coincidence peak is dominated by the (accidental) $K\alpha^N$ component, and inclusion of the $K\alpha^S$ component, which is shifted by only 88 eV (Ref. 27) from the $K\alpha^N$ line, would have very little effect on the resultant fit. The positions and widths of the four peaks, as well as the relative intensities of the α_2 to α_1 lines, were all fixed to the values shown in Table II. The centroids and widths of the $K\alpha_1^N$ and $K\alpha_2^N$ components were fixed

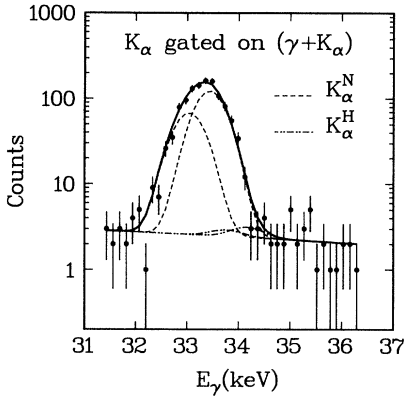

FIG. 5. The $K\alpha$ region of the coincidence spectrum gated on $(\gamma + K\alpha)$. The solid curve shows the overall fit to the data; the dashed curves show the $K\alpha_2^N$ and $K\alpha_1^N$ components and the dash-two-dots curves show the $K\alpha_2^H$ and $K\alpha_1^H$ components, each superimposed on a linear background.

to values extracted from fits to the $K\alpha^N \otimes K\alpha^N$ peak; the energies of the $K\alpha_1^H$ and $K\alpha_2^H$ peaks were shifted by 721 eV from the corresponding $K\alpha^N$ centroids. This shift was obtained from a quadratic fit to all the experimentally measured shifts of $K\alpha_1^H$ x ray lines, as a function of Z. Since this shift is somewhat larger than the 692 eV predicted by Chen, Crasemann, and Mark,[23] we also made fits in which the centroids of the $K\alpha^H$ peaks were varied by as much as ±50 eV from the above value. The yields were the same to within ±10%, a variation which is much smaller than the statistical error. The ratio of the $K\alpha_1^N$ to $K\alpha_2^N$ lines was taken as 1.84 (Ref. 24). Åberg *et al.*[25] have pointed out, however, that this ratio decreases for $K\alpha^H$ x rays, with its value being about 1.62 for La hypersatellite x rays.

The sensitivity of the extracted $K\alpha^H$ yield to the small Lorentzian broadening of the Gaussian line shape due to the short atomic lifetime was also investigated. A fit using a Voigt profile[28,29] with the width of the Lorentzian component fixed to the experimental value[30] was performed. The extracted yield of the $K\alpha^H$ component using the Voigt profile differed from that using a simple Gaussian by less than 10%, a variation which is well within the statistical error. The lack of sensitivity of our data to the Lorentzian broadening is due to the broad

TABLE II. Fixed parameters used in the fit to the $K\alpha$ peak in coincidence with $\gamma + K\alpha$, and the resultant areas.

Component	E (keV)	FWHM (keV)	Rel. Intensity	Total Area
$K\alpha_2^N$	33.034	0.715	1.00	
$K\alpha_1^N$	33.442	0.715	1.84	1114±35
$K\alpha_2^H$	33.755	0.715	1.00	
$K\alpha_1^H$	34.163	0.715	1.62	7±12

TABLE III. Fixed parameters used in the fit to the $K\alpha + K\alpha$ peak in coincidence with γ, and the resultant areas.

Component	E (keV)	FWHM (keV)	Rel. Intensity	Total Area
$K\alpha_2^N + K\alpha_2^N$	66.068	0.746	1.00	
$K\alpha_1^N + K\alpha_2^N$	66.476	0.746	3.68	226±20
$K\alpha_1^N + K\alpha_1^N$	66.884	0.746	3.38	
$K\alpha_2^S + K\alpha_2^H$	66.877	0.746	1.00	
$K\alpha_1^S + K\alpha_2^H$	67.285	0.746	3.46	17±14
$K\alpha_1^S + K\alpha_1^H$	67.693	0.746	2.98	

energy resolution of the detectors (715 eV), compared to the natural linewidth (17 eV), and due to the limited statistics in the fitted region.

The $(K\alpha + K\alpha)$ region of the spectrum gated on 166-keV γ rays will contain the accidental $(K\alpha^N + K\alpha^N)$ sum peak as well as the sought after $(K\alpha^S + K\alpha^H)$ sum peak (Fig. 6). Each of these sum peaks will consist of three components: $(K\alpha_2 + K\alpha_2)$, $(K\alpha_1 + K\alpha_2)$, and $(K\alpha_1 + K\alpha_1)$. [We ignore here the very small predicted[23] difference in energy (~ 7 eV) between the $(K\alpha_1^S + K\alpha_2^H)$ and $(K\alpha_2^S + K\alpha_1^H)$ sum peaks.] Since there is no angular correlation between the two $K\alpha$ x rays, the relative intensities of the three components can be obtained in a straightforward manner from the relative intensities $(K\alpha_1/K\alpha_2)^N = (K\alpha_1/K\alpha_2)^S = 1.84$ and $(K\alpha_1/K\alpha_2)^H = 1.62$. The width of a sum peak was taken to be the same as that of a single photon at the summed energy. Fits to true $[K\alpha(\mathrm{EC}) + K\alpha(\mathrm{IC})]$ sum coincidences in the singles spectrum with such an assumed width gave excellent results. Figure 6 shows the fit to the γ-gated $(K\alpha + K\alpha)$ region. Table III shows the peak positions, widths, and relative intensities used in the fit, and the resultant yields.

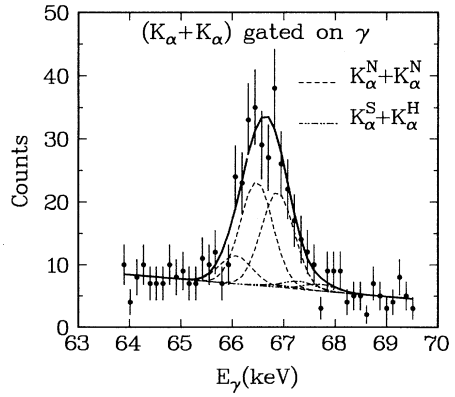

FIG. 6. The $K\alpha + K\alpha$ region of the coincidence spectrum gated on γ. The solid curve shows the overall fit to the data; the dashed curves show the $K\alpha_2^N + K\alpha_2^N$, $K\alpha_2^N + K\alpha_1^N$, and $K\alpha_1^N + K\alpha_1^N$ components, the dash-two-dots curves show the $K\alpha_2^S + K\alpha_2^H$, $K\alpha_2^S + K\alpha_1^H$, and $K\alpha_1^S + K\alpha_1^H$ components, each superimposed on a linear background.

The yield of $K\alpha^H$ could also be extracted from the $(\gamma + K\alpha^H)$ sum peak in the spectrum gated on $K\alpha^S$. This yield is, in principle, statistically independent from the yield of $K\alpha^H$ extracted from the spectrum gated on $(\gamma + K\alpha^S)$. However, as Fig. 5 and Table II show, the error on the (essentially null) $K\alpha^H$ yield extracted from $K\alpha^H \otimes (\gamma + K\alpha^S)$ coincidences is dominated by the high-energy tail of the $K\alpha^N$ peak from accidental (pileup) $K\alpha^N \otimes (\gamma + K\alpha^N)$ coincidences. The same accidental coincidences would appear in the $(\gamma + K\alpha^N)$ sum peak gated on $K\alpha$, and hence, to the extent the error on the extracted $(\gamma + K\alpha^H)$ yield is dominated by the tail of the accidental $(\gamma + K\alpha^N)$ peak, the yields of $K\alpha^H$ x rays extracted from the two spectra are *not* statistically independent. Further, the accidental $(\gamma + K\alpha^N)$ peak was dominated by pileup sums and hence its shape was not a pure Gaussian, but had a considerable low-energy tail which could not be simulated reliably. For these reasons, we chose not to include the yield of $K\alpha^H$ extracted from the $(\gamma + K\alpha^H)$ peak in our final result.

The efficiency of each detector was determined from the singles spectra by comparing the area of the $166 + K\alpha$ sum peak to the total (i.e., photopeak plus everything summing with the photopeak) yield of 166-keV γ rays in the spectrum:

$$N(166 + K\alpha) = N(166)\, P_K\, \omega_K\, (K\alpha/K_T)\, \epsilon_{K\alpha} \qquad (4)$$

The extracted photopeak efficiencies for $K\alpha$ x rays ranged from 0.227 to 0.278, depending on the detector

TABLE IV. Data relevant to the calculation of P_{KK}.

		$10^6 P_{KK}$
ω_K[a]	0.906	
$(K\alpha/K_T)$[a]	0.807	
$\epsilon_{K\alpha}$	0.227 – 0.278	
$N(\gamma \otimes K\alpha^N) \times 10^{-6}$ [b]	30.9±0.3	
$N[\gamma \otimes (K\alpha^S + K\alpha^H)]$	7±12	1.3±2.1
$N[(\gamma + K\alpha^S) \otimes K\alpha^H)]$	17±14	3.1±2.5
Weighted Average		2.0±1.6

[a] Reference 24.

[b] This is the sum of all $\gamma \otimes K\alpha$ coincidences.

in question and the position of the source.

From the yield of $K\alpha^H \otimes (\gamma + K\alpha^S)$ coincidences we deduce a P_{KK} of $(1.3 \pm 2.1) \times 10^{-6}$, while from the yield of $\gamma \otimes (K\alpha^H + K\alpha^S)$ coincidences we deduce a P_{KK} of $(3.1 \pm 2.5) \times 10^{-6}$, for a weighted average of $(2.0 \pm 1.6) \times 10^{-6}$. The results are summarized in Table IV.

We also searched for the $K\alpha \otimes (K\alpha + K\alpha)$ coincidences that would result from double ionization accompanying IC of the 166-keV transition, but, as can be seen from the spectrum gated on $K\alpha$ in Fig. 4, the region of the $(K\alpha + K\alpha)$ sum peak in this spectrum is dominated by the Compton tail of the 166-keV γ ray and no meaningful yield for these triple coincidences could be extracted.

IV. DISCUSSION

Our result for P_{KK} is a factor of 5 smaller than the rough experimental value of $(1 \pm 1) \times 10^{-5}$ given by Schupp *et al.*,[21] and gives experimental justification to their neglect of the contribution of P_{KK}(EC) to their deduced value of P_{KK}(IC) of $(6.0 \pm 1.4) \times 10^{-5}$.

Unfortunately, our value of $(2.0 \pm 1.6) \times 10^{-6}$ is not sensitive enough to test the predictions of the Suzuki and Law theory (8.4×10^{-7}), or that of Intemann[22] (2.6×10^{-7}). Because the statistical error on our result is due primarily to the high-energy tail of accidental $K\alpha^N$ x rays, an improved statistical limit can only be achieved by counting for a longer time and/or by improving the detector resolution. To reduce the statistical error by a factor of 3 (using the same detectors) would require a counting time of 27 months. Clearly, a better solution would be to obtain detectors with better resolution. Nevertheless, the result is low enough to indicate that the SL predictions for EC decays with low Q values do not underestimate measured P_{KK}'s by the large factor of 9 ± 3 suggested by the higher of the two experimental values for ^{181}W (Table I).

Mukoyama, Isozumi, Kitahara, and Shimizu[2] (MIKS) did not make an explicit calculation of P_{KK} for ^{139}Ce. The expressions they use to calculate P_{KK} [Eqs. (17) and (32) in Ref. 2] depend on the screening constant σ, and a parameter ξ.[31–33] If we use $\sigma = 0.704$, by interpolating from Table I in Ref. 1 and $\xi = \frac{2}{3}$, a value that is comparable with values 0.687–0.862 used by Mukoyama *et al.*, we get P_{KK}(MIKS) $= 1.72 \times 10^{-5}$, which is about a factor of 9 larger than our measurement. Since P_{KK}(MIKS) depends sensitively on σ we have estimated P_{KK}(MIKS) for several values of σ, to see if it is possible to get a lower value of P_{KK}(MIKS) for a reasonable value of σ. To get P_{KK}(MIKS) $= 2.0 \times 10^{-6}$, the unreasonably large value of $\sigma = 0.90$ is required. P_{KK}(MIKS) depends linearly on ξ, so a value of $\xi = 0.07$ (at $\sigma = 0.704$) is required to make P_{KK}(MIKS) $= P_{KK}$(exp). We shall show below, using some rough approximations, that ξ could be as low as 0.37; whether it can be as low as 0.07 awaits a calculation identical to that performed by MIKS.

Our measurement for ^{139}Ce, combined with that of the neighboring Z isotope ^{131}Cs, allows us to make a rough estimate of the probability $P^{(0)}$ of leaving zero holes in the K shell per K capture. This can occur via the shakedown of higher orbit electrons to the K shell. Since the shakedown of an electron from the ns shell leaves the system (atom + neutrino) in a state indistinguishable from that produced during direct capture from the ns shell, the process is virtually impossible to detect directly. We rely therefore on the connection between P_{KK} and $P^{(0)}$:[31,32]

$$P_{KK} \equiv P^{(2)} = 1 - P^{(1)} - P^{(0)}, \tag{5}$$

where $P^{(1)}$ is the probability, per K capture, of leaving one hole in the K shell. Using a notation similar to that of MIKS,[2] $P^{(1)}$ and $P^{(0)}$ are given by

$$P^{(1)} = |\langle \psi_f(Z', K) | \psi_i(Z, K) \rangle|^2 , \tag{6}$$

$$P^{(0)} = \sum_{n=2}^{n'} (Q_n/Q_0)^2 |\langle \psi_f(Z', K) | \psi_i(Z, n) \rangle|^2 , \tag{7}$$

where $\langle \psi_f(Z', K) | \psi_i(Z, n) \rangle$ is the atomic-wave-function overlap of the ns state of the parent atom with the $1s$ state of the daughter atom; Q_0 is the energy released in K capture:

$$Q_0 = m_i - m_f - B_K , \tag{8}$$

with m_i and m_f being the initial and final atomic masses, respectively, and B_K the K-shell binding energy in the daughter atom. The expression for Q_n, the energy released in K-capture accompanied by shakedown from the ns shell, is identical to Eq. (8), with B_K replaced by B_n, the binding energy of an electron in the ns state of the daughter atom. Since $(Q_n/Q_0)^2$ increases by only 14% as n increases from 2 to ∞, and since the matrix elements decrease rapidly with n,[31] we can make the reasonable approximation

$$\begin{aligned} P^{(0)} &\simeq (Q_2/Q_0)^2 \sum_{n=2}^{n'} |\langle \psi_f(Z', K) | \psi_i(Z, n) \rangle|^2 \\ &\equiv (Q_2/Q_0)^2 \, M^{SD} , \end{aligned} \tag{9}$$

where M^{SD} was introduced as a shorthand for the sum over the squares of the shakedown matrix elements. With this approximation the difference between the P_{KK}'s of ^{131}Cs and ^{139}Ce can be written as

$$\begin{aligned} P^{(2)}_{\rm Cs} - P^{(2)}_{\rm Ce} = P^{(1)}_{\rm Ce} - P^{(1)}_{\rm Cs} &+ (Q_2/Q_0)^2_{\rm Ce} \, M^{SD}_{\rm Ce} \\ &- (Q_2/Q_0)^2_{\rm Cs} \, M^{SD}_{\rm Cs} . \end{aligned} \tag{10}$$

Now we make the approximation $M^{SD}_{\rm Ce} \cong M^{SD}_{\rm Cs}$. Since for ^{139}Ce $Z = 58$, and for ^{131}Cs $Z = 55$, this approximation should be a reasonably good one. Two of the extra three electrons that Ce possesses are in the $4f$ and $5d$ shells, and hence do not contribute to M^{SD}, and the third one is in the $6s$ shell, and hence has a much smaller overlap with the $1s$ state than the $2s$–$5s$ electrons do. The difference between $M^{SD}_{\rm Ce}$ and $M^{SD}_{\rm Cs}$ then comes primarily from the Z dependence of the matrix elements. This dependence is expected[31] to go as $1/Z^2$ and hence

$M^{SD}_{Cs}/M^{SD}_{Ce} \cong (58/55)^2 = 1.11$. Taking this ratio to be unity, Eq. (10) becomes

$$P^{(2)}_{Cs} - P^{(2)}_{Ce} = P^{(1)}_{Ce} - P^{(1)}_{Cs} + [\,(Q_2/Q_0)^2_{Ce} - (Q_2/Q_0)^2_{Cs}]M^{SD}_{Ce}\ . \quad (11)$$

Now, $P^{(1)}$ increases[31] with Z, so an overestimate of M^{SD} can be obtained from Eq. (11) by assuming $P^{(1)}_{Ce} = P^{(1)}_{Cs}$. Using the experimentally measured values of $P^{(2)}_{Cs} = (1.4 \pm 0.1) \times 10^{-5}$ (Ref. 18), $P^{(2)}_{Ce} = (2.0 \pm 1.6) \times 10^{-6}$ (this work), $Q_{EC} = 265 \pm 5$ keV for ^{139}Ce decay,[24] $Q_{EC} = 347 \pm 5$ keV for ^{131}Cs decay,[34] and electron binding energies from Ref. 24, one obtains $M^{SD} \lesssim (1.02 \pm 0.20) \times 10^{-5}$. (The quoted uncertainty on M^{SD} reflects only the propagated errors on the measured values of $P^{(2)}$ and the Q values, not the approximations.) From this value of M^{SD} we deduce $P^{(0)}_{Ce} \lesssim 2.4 \times 10^{-5}$ and $P^{(0)}_{Cs} \lesssim 1.2 \times 10^{-5}$.

A value for $P^{(0)}_{Cs}$ can be inferred from the MIKS calculation as follows: Since

$$P^{(2)} = 1 - P^{(1)} - P^{(0)} \equiv \xi\,(1 - P^{(1)})\ , \quad (12)$$

then

$$P^{(0)} = P^{(2)}\,\frac{1-\xi}{\xi}\ ; \quad (13)$$

using the MIKS values[2] $\xi = 0.687$ and $P^{(2)} = 1.79 \times 10^{-5}$, we get $P^{(0)} = 0.82 \times 10^{-5}$, which compares favorably with our upper experimental estimate ($P^{(0)}_{Cs} \lesssim 1.2 \times 10^{-5}$). If, rather than make the approximation $P^{(1)}_{Ce} = P^{(1)}_{Cs}$, we calculate this difference from the MIKS expression for $P^{(1)}$, and take $M^{SD}_{Cs} = 1.1 M^{SD}_{Ce}$ we get "experimental" estimates of $P^{(0)}_{Cs} = 1.1 \times 10^{-5}$ and $P^{(0)}_{Ce} = 2.0 \times 10^{-5}$.

We would like to emphasize here the fortuitous circumstances which made an experimental deduction of $P^{(0)}$ possible: (1) the knowledge of $P^{(2)}$ for two neighboring atoms where $\Delta Z/Z$ is small enough to make the approximation of the equality of the matrix elements a reasonable one, and (2) values of $(Q_2/Q_0)^2$ which are sufficiently different for the two decays to make Eq. (11) sensitive to M^{SD}. In addition to the ^{131}Cs-^{139}Ce pair, a similar situation exists for the ^{103}Pd-^{109}Cd pair, where we find $P^{(0)}_{Pd} = (3.5 \pm 0.8) \times 10^{-5}$ and $P^{(0)}_{Cd} = (5.6 \pm 1.3) \times 10^{-5}$.

Next we return to the question of ξ for the ^{139}Ce decay. If we deduce M^{SD}_{Cs} from the MIKS calculation for ^{131}Cs and assume $M^{SD}_{Ce} = M^{SD}_{Cs}/1.11$, we get $\xi_{Ce} = 0.43$. Here $P^{(1)}$ was calculated with $\sigma = 0.704$. If we use $\sigma = 0.720$ we get $\xi_{Ce} = 0.37$. While these values of ξ are substantially lower than the values 0.687–0.862 that were found by MIKS for other isotopes, they still lead to values of P_{KK} (1.1×10^{-5} for $\sigma = 0.704$ and 0.84×10^{-5} for $\sigma = 0.720$) which are at least a factor of 4 larger than our measurement. However, in the case of ^{139}Ce, $P^{(0)}$ is of the same order as $(1 - P^{(1)})$; thus, the value of ξ, and hence $P^{(2)}$, depends sensitively on $P^{(0)}$, and the approximation $M^{SD}_{Ce} = M^{SD}_{Cs}/1.11$, which might be adequate for determining $P^{(0)}$ itself, might not be adequate in determining the *difference* between $P^{(0)}$ and $1 - P^{(1)}$. Therefore, without an explicit calculation of ξ_{Ce}, it is not possible to make a definitive comparison between our result and the prediction of the MIKS model.

To summarize, we have determined P_{KK}(EC) for ^{139}Ce decay to be $(2.0 \pm 1.6) \times 10^{-6}$. While this value is not sensitive enough to test the predictions of Intemann and Suzuki and Law,[22] it is sufficiently small to indicate that the triple coincidences recorded between $K\alpha^N$, $K\alpha^S$, and $K\alpha^H$ x rays in the experiment of Schupp, Nagy, and Miles[21] are indeed dominated by double ionization accompanying the internal conversion of the 166-keV transition. By combining our measured value of P_{KK} with that for the neighboring (in Z) isotope ^{131}Cs, we estimate $P^{(0)}$ to be $\lesssim 2.4 \times 10^{-5}$ for ^{139}Ce and $\lesssim 1.2 \times 10^{-5}$ for ^{131}Cs.

ACKNOWLEDGMENTS

The assistance of Randy Bybee and Alan Helfer in collecting the data is gratefully acknowledged, as is the assistance of Dr. Paul Semmes in preparing sources. The loan of electronic modules by Dr. Peter Parker of Yale University is deeply appreciated. We thank Dr. G. Schupp for providing us with the computer code for calculating the Voigt profile. This work was supported by the U.S. Department of Energy, Nuclear Physics Division, via Grant No. DE-FG05-87ER40314.

[1] R.L. Intemann, Phys. Rev. C **31**, 1961 (1985).
[2] T. Mukoyama, Y. Isozumi, T. Kitahara, and S. Shimizu, Phys. Rev. C **8**, 1308 (1973).
[3] A. Suzuki and J. Law, Phys. Rev. C **25**, 514 (1982).
[4] R.W. Kiser and W.H. Johnston, J. Am. Chem. Soc. **81**, 1810 (1959).
[5] H.J. Nagy and G. Schupp, Phys. Rev. C **30**, 2031 (1984).
[6] J.P. Briand, P. Chevalier, A. Johnson, J.P. Rozet, M. Tavernier, and A. Touati, Phys. Lett. **49A**, 51 (1974).
[7] T. Kitahara and S. Shimizu, Phys. Rev. C **11**, 920 (1975).
[8] H.J. Nagy and G. Schupp, Phys. Rev. C **27**, 2887 (1983).
[9] J.P. Briand, P. Chevalier, M. Tavernier, and J.P. Rozet, Phys. Rev. Lett. **27**, 777 (1971).
[10] G. Schupp and H.J. Nagy, Phys. Rev. C **29**, 1414 (1984).
[11] C.W.E. van Eijk, J. Wijnhorst, and M.A. Popelier, Phys. Rev. A **20**, 1749 (1979).
[12] H.J. Nagy, G. Schupp, and R.R. Hurst, Phys. Rev. C **11**, 205 (1975).
[13] C.W.E. van Eijk and J. Wijnhorst, Phys. Rev. C **15**, 1068 (1977).
[14] C.W.E. van Eijk, J. Wijnhorst, and M.A. Popelier, Phys. Rev. C **19**, 1047 (1979).
[15] P. Venugopala Rao, I.J. Unus, P.A. Indira, Ali M. Guima, and V.R. Veluri, International Conference on X-ray and Atomic Inner-Shell Physics, Eugene, Oregon, 1982 (unpublished).

[16] H.J. Nagy, G. Schupp, and R.R. Hurst, Phys. Rev. C **6**, 607 (1972).
[17] R.J. Walen, CNRS Report No. 1976/77, 1976 (unpublished).
[18] Y. Isozumi, Ch. Briançon, and R.J. Walen, Phys. Rev. C **25**, 3078 (1982).
[19] C.W.E. van Eijk, J.P. Wagenaar, F. Bergsma, and W. Lourens, Phys. Rev. A **26**, 2749 (1982).
[20] J.P. Briand, J.P. Rozet, P. Chevallier, A. Chetioui, M. Tavernier, and T. Touati, J. Phys. B **13**, 4751 (1980).
[21] G. Schupp, H.J. Nagy, and V.A. Miles, Phys. Rev. C **36**, 2533 (1987).
[22] Quoted in Ref. 21 as private communications from A. Suzuki and J. Law and from R.L. Intemann.
[23] M.H. Chen, B. Crasemann, and H. Mark, Phys. Rev. A **25**, 391 (1982).
[24] *Table of Isotopes*, 7th ed., edited by C.M. Lederer and Virginia S. Shirley (Wiley, New York, 1978).
[25] R. Åberg, J.P. Briand, A.P. Chevalier, A. Chetioui, J.P. Rozet, M. Tavernier, and A. Touati, J. Phys. B **9**, 2815 (1976).
[26] W. Bambynek, H. Behrens, M.H. Chen, B. Crasemann, M.L. Fitzpatrick, K.W.D. Ledingham, H. Genz, M. Mutterer, and R.L. Intemann, Rev. Mod. Phys. **49**, 77 (1977).
[27] D. Burch, L. Wilets and W.E. Meyerhof, Phys. Rev. A **9**, 1007 (1974).
[28] R. Gunnink, Nucl. Instrum. Methods **143**, 145 (1977).
[29] M. Mori, Publ. Res. Inst. Math. Sci. **19**, 1081 (1983).
[30] S. I. Salem and P. L. Lee, At. Data Nucl. Data Tables **18**, 233 (1976).
[31] H. Primakoff and F.T. Porter, Phys. Rev. **89**, 930 (1953).
[32] J.S. Levinger, Phys. Rev. **90**, 11 (1953).
[33] T.A. Carlson, C.W. Nestor, Jr., T.C. Tucker, and F.B. Malik, Phys. Rev. **169**, 27 (1968).
[34] A.H. Wapstra and G. Audi , Nucl. Phys. **A432**, 1 (1985).